THE JOURNAL OF BIOLOGICAL CHEMISTRY VOL. 288, NO. 9, pp. 6542–6551, March 1, 2013

The Free Fatty Acid Receptor G Protein-coupled Receptor 40 (GPR40) Protects from Bone Loss through Inhibition of Osteoclast Differentiation*

Received for publication, October 29, 2012, and in revised form, December 5, 2012 Published, JBC Papers in Press, January 18, 2013, DOI 10.1074/jbc.M112.429084

Fabien Wauquier[‡§¶], Claire Philippe[‡§¶], Laurent Léotoing[‡§¶], Sylvie Mercier[‡§¶], Marie-Jeanne Davicco[‡§¶], Patrice Lebecque[‡§¶], Jérôme Guicheux[‖], Paul Pilet[‖**], Elisabeth Miot-Noirault[§‡‡], Vincent Poitout[§§¶¶1], Thierry Alquier[§§¶¶2], Véronique Coxam[‡§¶], and Yohann Wittrant[‡§¶3]**

*From the [‡]Institut National de la Recherche Agronomique, Unité Mixte de Recherche 1019, Unité de Nutrition Humaine, Centre de Recherche en Nutrition Humaine Auvergne, F-63009 Clermont-Ferrand, France, [§]Clermont Université, Université d'Auvergne, Unité de Nutrition Humaine, BP 10448, F-63000 Clermont-Ferrand, France, [¶]Equipe Alimentation, Squelette et Métabolismes and [‖]Institut National de la Santé et de la Recherche Médicale, UMR S791, Laboratoire d'Ingénierie Ostéo-Articulaire et Dentaire, F-44042 Nantes, France, **Pôle de Recherche et d'Enseignement Supérieur Université Nantes Angers Le Mans, Université de Nantes, Unité de Formation et de Recherche Odontologie, 1 Place Alexis Ricordeau, F-44042 Nantes, France, [‡‡]INSERM, UMR 990, F-63000 Clermont-Ferrand, France, [§§]Centre de Recherche du Diabète de Montréal, Centre de Recherche du Centre Hospitalier de l'Université de Montréal (CRCHUM) and [¶¶]Département de Médecine, Université de Montréal, Montréal, Quebec H3T 1J4, Canada*

Background: Long chain fatty acids have been shown to activate the membrane-bound receptor GPR40.
Results: GPR40 agonist alters bone-resorbing cell differentiation through inhibition of the NF-κB system.
Conclusion: GPR40 exerts protective effects *in vivo* on bone tissue.
Significance: GPR40 is a nutritional and therapeutic target opening up new avenues for clinical investigations in terms of metabolic and age-related bone disorders.

The mechanisms linking fat intake to bone loss remain unclear. By demonstrating the expression of the free fatty acid receptor G-coupled protein receptor 40 (GPR40) in bone cells, we hypothesized that this receptor may play a role in mediating the effects of fatty acids on bone remodeling. Using micro-CT analysis, we showed that GPR40$^{-/-}$ mice exhibit osteoporotic features suggesting a positive role of GPR40 on bone density. In primary cultures of bone marrow, we showed that GW9508, a GRP40 agonist, abolished bone-resorbing cell differentiation. This alteration of the receptor activator of NF-κB ligand (RANKL)-induced osteoclast differentiation occurred via the inhibition of the nuclear factor κB (NF-κB) signaling pathway as demonstrated by decrease in gene reporter activity, inhibitor of κB kinase (IKKα/β) activation, inhibitor of κB (IkBα) phosphorylation, and nuclear factor of activated T cells 1 (NFATc1) expression. The GPR40-dependent effect of GW9508 was confirmed using shRNA interference in osteoclast precursors and GPR40$^{-/-}$ primary cell cultures. In addition, *in vivo* administration of GW9508 counteracted ovariectomy-induced bone loss in wild-type but not GPR40$^{-/-}$ mice, enlightening the obligatory role of the GPR40 receptor. Then, in a context of growing prevalence of metabolic and age-related bone disorders, our results demonstrate for the first time in translational approaches that GPR40 is a relevant target for the design of new nutritional and therapeutic strategies to counter bone complications.

Dietary lipid intake has been linked to inflammation, which itself is a key player involved in bone resorption and osteoporosis (1, 2). Inflammation favors bone degradation by stimulating osteoclast activity while inhibiting osteoblast-mediated bone formation, leading to unbalanced bone remodeling and subsequent bone loss. Dietary lipids have been reported to exert dual effects on inflammation, with both pro- and anti-inflammatory effects depending on their structure and metabolism (3, 4). In this regard, a growing body of evidence suggests that ω-6 fatty-acids promote bone loss, whereas ω-3 fatty acids restrain it (1, 2, 5, 6). However, the effects of fatty acids on bone density remain controversial and the underlying mechanisms of action poorly understood. More specifically, whether or not fatty acid receptors of the peroxisome proliferator-activated receptor (PPAR),[4] Toll-like receptor (TLR), or G protein-coupled receptor families are implicated in these effects remains uncertain.

Diascro *et al.* were the first to demonstrate that a mixture of palmitic, oleic, and linoleic acids activates PPARs to drive adipocyte-like differentiation of both ROS17/2.8 and SaOS-2/B10 preosteoblast cell lines (7). At the cellular and molecular levels, PPARγ activation was shown to reduce expression and func-

* This work was supported in part by the Canadian Institutes of Health Research Grant MOP 177381 (to V. P.).
[1] Holds the Canada Research Chair in Diabetes and Pancreatic Beta-cell Function.
[2] Supported by a postdoctoral fellowship from the Canadian Diabetes Association.
[3] To whom correspondence should be addressed: INRA, UMR 1019, UNH, CRNH Auvergne, Clermont Université, Université d'Auvergne, Unité de Nutrition Humaine, BP 10448, F-63000 Clermont-Ferrand, France. Tel.: 33-473-624-784; Fax: 33-957-059-912; E-mail: yohann.wittrant@clermont.inra.fr.

[4] The abbreviations used are: PPAR, peroxisome proliferator-activated receptor; DMSO, dimethyl sulfoxide; OVX, ovariectomy; RANKL, receptor activator of NF-κB Ligand; TLDA, Taqman low density array; TLR, Toll-like receptor; TRACP, tartrate-resistant acid phosphatase.

tion of Runx2, a transcription factor inducing osteoblastogenesis (8, 9). These data support the notion that fatty acid intake may have a strong impact on bone metabolism. TLRs were recently shown to bind saturated fatty acid (10) and to be involved in fatty-acid induced insulin resistance (11–13). Relevant to bone metabolism, mice deficient for TLR4 exhibit increased bone size with increased bone mineral content and density (14).

In 2003, Briscoe *et al.* (15), Itoh *et al.* (16), and Kotarsky *et al.* (17) demonstrated that the previously orphan G protein-coupled receptor GPR40 was expressed at high levels in pancreatic beta cells and was able to interact with medium to long chain fatty acids. Subsequently, the role of GPR40 (also known as free fatty acid receptor-1/FFAR-1) was mainly examined in beta cells for its involvement in insulin secretion (18). Using GPR40-deficient mice, we showed that GPR40 contributes to fatty acid potentiation of glucose-induced insulin secretion (19). Indeed, the ability of GPR40 to enhance insulin release only when glucose levels are elevated made it an appealing drug target for the treatment of type 2 diabetes, and agonists of GPR40 have shown very encouraging results in recent phase 2 clinical trials (20, 21).

In addition to the pancreatic beta cell, expression of free fatty acid receptors was also documented in leukocytes and monocytes (22, 23). As bone tissues share common precursor cells with the hematopoietic lineage, GPR40 expression was investigated in bone cells (24, 25). Indirect evidence in support for a role of GPR40 in fatty acid stimulation of bone formation was provided by Cornish *et al.*, who observed that GPR40 is expressed in osteoclasts and that a GPR40 agonist mimics fatty acid inhibition of osteoclastogenesis (24). Mieczkowska *et al.* recently confirmed the expression of GPR40 in bone cells and observed that down-regulation of GPR40 by RNA interference protects from thiazolidinedione-induced osteocyte apoptosis (25). In view of these seemingly conflicting results, our study was aimed to further determine the impact of GPR40 deletion on bone density and osteoclastogenesis in mice. Our results demonstrate that GPR40 is a key modulator of bone remodeling by counteracting osteoclast-mediated bone loss. These findings suggest that GPR40 agonists, currently under development for the treatment of type 2 diabetes, could have additional beneficial effects on the prevention of osteoporosis.

EXPERIMENTAL PROCEDURES

Ethics

All animal procedures were approved by the institution's animal welfare committee (Comité d'Ethique en Matière d'Expérimentation Animale Auvergne: CEMEAA) and were conducted in accordance with the European guidelines for the care and use of laboratory animals (2010-63UE). Animals were housed in the animal facility of the INRA Research for Human Nutrition (Agreement C6334514). All surgeries were performed under anesthesia, and all efforts were made to minimize suffering.

Animals

GPR40$^{-/-}$ Mice—GPR40$^{-/-}$ mice were obtained from AMGEN Inc. As described by Latour *et al.* (19), GPR40$^{-/-}$ mice on a mixed C57BL/6/129 background were generated by homologous recombination in embryonic stem cells at Lexicon Genetics (The Woodlands, TX). Exon 2 of the GPR40 gene was replaced with a LacZ gene. The mice were backcrossed onto the C57BL/6 strain over nine generations. Pups were screened by PCR performed on genomic DNA. Wild-type (WT) littermates were used as controls.

Ovariectomized Mice—After an acclimatization period, 9-week-old female mice were subjected to ovariectomy (OVX). After surgery, mice were housed one per cage for the total duration of the experiment and randomly divided into distinct groups ($n = 7$ per group; wild-type or GPR40$^{-/-}$: sham-operated/control vehicle; OVX/control vehicle; OVX/GW9508). Gavage was started after a 24-h recovery period. Three times per week mice received 100 μl of either DMSO as control vehicle or GW9508 (Cayman Chemical CAS 885101-89-3) at a concentration of 8 mg/kg of body weight for 5 weeks.

Bone Microarchitecture and Bone Mineral Density Analyses

After removing soft tissues, left femurs were placed in PBS buffer with 10% formaldehyde at 4 °C for 1 week. Microarchitecture (secondary spongiosa) was analyzed using x-ray radiation micro-CT (SkyScan 1072). Pictures of 1024*1024 pixels were obtained using 37 kV and 215 μA. Bone mineral density analysis was done using an eXplore CT 120 scanner (GE Healthcare). Acquisitions were performed with x-ray tube settings at 100 kV and 50 mA.

Body Mass and Composition

Mice were weighed every week throughout the experimental period and subjected to body composition analyses at the beginning and at the end of the protocol using QMR EchoMRI-900^{TM} system. Whole body fat and lean mass were measured in live animals without anesthesia or sedation.

Primary Bone Marrow Cultures for Osteoclast Formation

Bone marrow cells were isolated from femurs marrow cavity excised from 3–5-week-old wild-type or GPR40$^{-/-}$ male mice. Cells were washed and plated in α-MEM supplemented with 10% FCS at a density of $2.5*10^6$ cells/cm^2. Cultures were grown either in complete medium alone (control) or in differentiation medium (recombinant murine-receptor activator of NF-κB ligand (RANKL) (50 ng/ml) (R & D Systems)) in the presence or absence of GW9508. Culture media were changed every 2 days. On day 6, cultures were harvested for analyses.

RAW264.7 Cultures

The murine osteoclast precursor cell line RAW264.7 was obtained from the American Type Culture Collection (ATCC TIB-71). For osteoclast differentiation experiments, cells were seeded at a density of $3*10^4$ cells/cm^2 and grown as described for bone marrow cultures. For signaling experiments, cells were serum-starved for 48 h for each condition.

Cell Viability Assays

RAW264.7 cells were seeded in a 96-well plate at a density of 3500 cells/well and cultured for 24 h supplemented with 2% serum in the presence of vehicle (DMSO) or 10–100 μM of GW9508. The cell viability was determined by an XTT-based

A.

	WT	GPR 40-/-
BV/TV (%)	22.497 ± 4.576	17.886 ± 4.518 *
Tb.Th (mm)	0.158 ± 0.016	0.130 ± 0.039 *
Tb.N (1/mm)	1.425 ± 0.287	1.462 ± 0.526
Tb.Sp (mm)	0.179 ± 0.073	0.193 ± 0.036
Bone surface density (1/mm)	10.843 ± 1.664	9.233 ± 1.207*

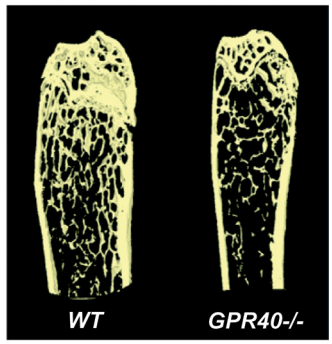

B.

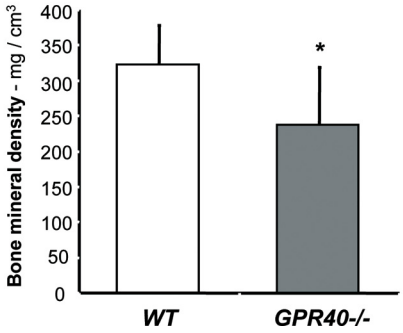

C.

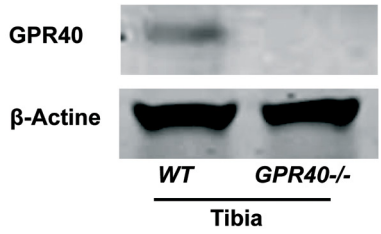

FIGURE 1. **GPR40$^{-/-}$ mice exhibit an osteoporotic phenotype.** *A*, micro-CT analysis with corresponding images of left femurs from wild-type (WT) and GRP40$^{-/-}$ mice (males; 16 weeks old mice; $n = 11$/group; *BV/TV*, bone volume/total volume; *Tb.N*, trabecular number; *Tb.Sp*, trabecular spaces; *Tb.Th*, trabecular thickness). *B*, bone mineral density. *C*, Western blot analysis of GPR40 expression in bone (tibia). *Error bars* represent standard deviation (±S.D.); *, $p < 0.05$.

method, using the Cell Viability/Proliferation Kit II (Sigma-Aldrich) according to the supplier's recommendations. The absorbance was determined at 450 nm.

Tartrate-resistant Acid Phosphatase (TRACP) Assays

Enzymatic Activity—TRACP activity was measured according to standard methods using *p*-nitrophenyl phosphate as a substrate (26). Medium was removed, and cell lysates were prepared using Nonidet P-40 lysis buffer. Samples were incubated in assay buffer (125 mM sodium acetate buffer (pH 5.2), 100 mM *p*-nitrophenyl phosphate (Sigma-Aldrich), and 1 mM L(+) sodium tartrate). The production of *p*-nitrophenol was determined at 405 nm at 37 °C and expressed as the mean absorbance/minute per milligram of proteins.

Cell Staining—In parallel experiments, cellular TRACP activity was analyzed using the leukocyte acid phosphatase kit (Sigma-Aldrich). Briefly, the cells were washed twice with PBS, fixed for 5 min with citrate/paraformaldehyde/acetone solution, and stained according to the manufacturer's instructions.

Cell Transfection and NF-κB-dependent Luciferase Activity

RAW264.7 cells were transfected at ~80% confluence with 80 ng/cm^2 of NF-κB-RE/pGL3 Basic-luciferase vector using FuGENE HD transfection reagent (Roche Applied Science) according to published methods (26). 24 h after transfection, cells were incubated with RANKL (50 ng/ml) in the presence of vehicle (DMSO) or 50 μM GW9508. At 6 and 24 h after treatment, cell lysates were prepared, and luciferase activity was quantified using the luciferase assay kit (Promega). For each condition, data are expressed as relative light units/mg of proteins.

GPR40 Silencing

Long term GPR40 knockdown in RAW264.7 cells was obtained using the SureSilencing™ shRNA Interference technology (SABiosciences, Qiagen). After 1-month selection, growing cells were harvested for GPR40 expression by real-time RT-PCR. Colonies exhibiting the highest knockdown efficiency were selected for further investigations.

Western Blot Analysis

Bone tissues from wild-type and GPR40$^{-/-}$ mice as well as cultured cells were lysed and subjected to Western blot analysis. Tissues and cultured cells were immediately chilled on ice and lysed for 30 min using Nonidet P-40 lysis buffer. Proteins were quantified using BCA kit (Sigma-Aldrich) according to the manufacturer's protocol, and 20 μg of total protein was loaded and resolved on a 10% SDS-polyacrylamide gel and transferred to a nitrocellulose membrane (Invitrogen). GPR40, inhibitor of κB kinase-α (IKKα), phospho-IKKα/β (Ser$^{176/180}$), inhibitor of κBα (IkBα), phospho-IkBα (Ser^{32}), and β-actin were detected using specific antibodies from Santa Cruz Biotechnology (Santa Cruz, CA; GPR40: sc-28416/β-actin: sc-47778), and Cell Signaling Technology (2682, 2697, 4814, 2859), respectively. Proteins were revealed by chemiluminescence using ECL reagent (Amersham Biosciences).

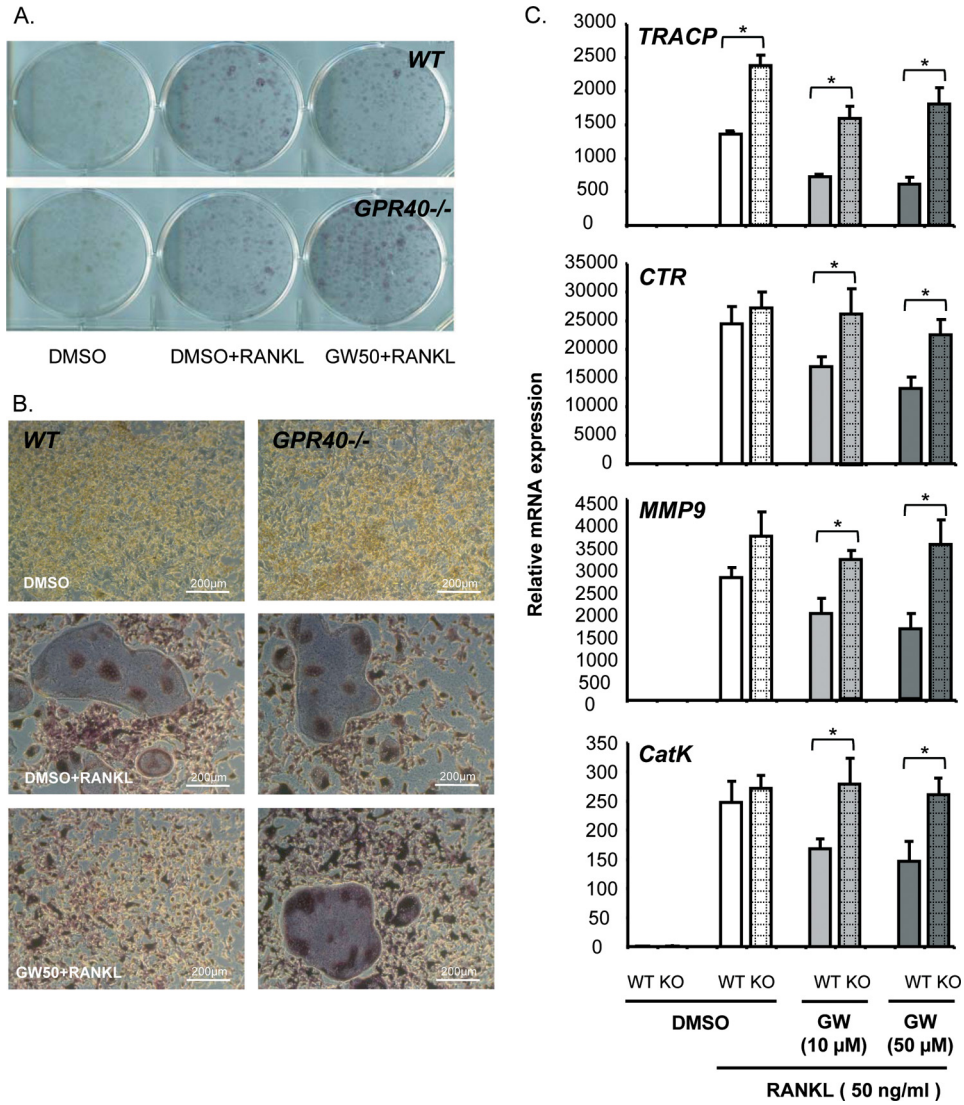

FIGURE 2. **GW9508 inhibits RANKL-induced osteoclast differentiation in primary cell cultures obtained from mouse bone marrow tissues.** *A* and *B*, TRACP staining: wild-type (WT) *versus* GPR40$^{-/-}$ mice (KO). Magnification, ×10 (Zeiss). Osteoclast differentiation was induced by murine recombinant RANKL (50 ng/ml). DMSO was used as a vehicle. GPR40 agonist GW9508 was used at either 10 or 50 μM (GW10 or GW50). *C*, osteoclast marker expression analyzed by real-time RT-PCR. *Error bars* represent standard deviation (±S.D.); *, $p < 0.05$.

Real-time RT-PCR

Total RNA was isolated using TRIzol reagent (Invitrogen) and treated with deoxyribonuclease I (1 unit/μg). RNA concentration was determined using Nanodrop technology. cDNA was obtained from 1 μg of total RNA using SuperScript VILO™ cDNA synthesis kit according to the manufacturer's protocol. RT reaction mixture was diluted 1/10 and subjected to PCR using specific primers (200 nM final each) and EXPRESS SYBR GreenER qPCR Supermix Universal according to the supplier's instructions. Primers were designed as following: cathepsin K (*CatK*) forward, cgaaaagagcctagcgaaca and reverse, tgggtagcagcagaaacttg; calcitonin receptor (*CTR*) forward, tgcgaggggatctatcttca and reverse, gttggcactatcgggaacc; *TRACP* forward, ccagcgacaagaggttcc and reverse, agagacgttgccaaggtgat; matrix metalloproteinase-9 (*MMP-9*) forward, cgacatagacggcatccag and reverse, ctgtcggctgtggttcagt; nuclear factor of activated T cells 1 (*NFATc1*) forward, gggtcagtgtgaccgaagat and reverse, ggaagtcagaagtgggtgga. Relative expression was calculated using the comparative ΔΔCt method. *GAPDH* and *18S* served as control. Data are expressed as relative mRNA expression. Control condition was arbitrarily set at 1.

Taqman Low Density Arrays (TLDAs)

At the end of the GW9508 administration period, left femurs from wild-type OVX mice were isolated and cleaned from any soft tissues. Samples were immediately frozen into liquid nitrogen and crushed into powder prior to RNA extraction (TRIzol) and RT. Resulting cDNA was used for TLDAs (Applied Biosystems 7900HT real-time PCR system). Relative expression values were calculated using the comparative threshold cycle ($2^{-\Delta\Delta CT}$) according to Data Assist software (Applied Biosystems). 18S, GAPDH, and actin served as housekeeping genes.

Statistics

Data obtained were analyzed either by ANOVA Fisher's (two groups) or Newman's Kell (>two groups) test (ExcelStat Pro

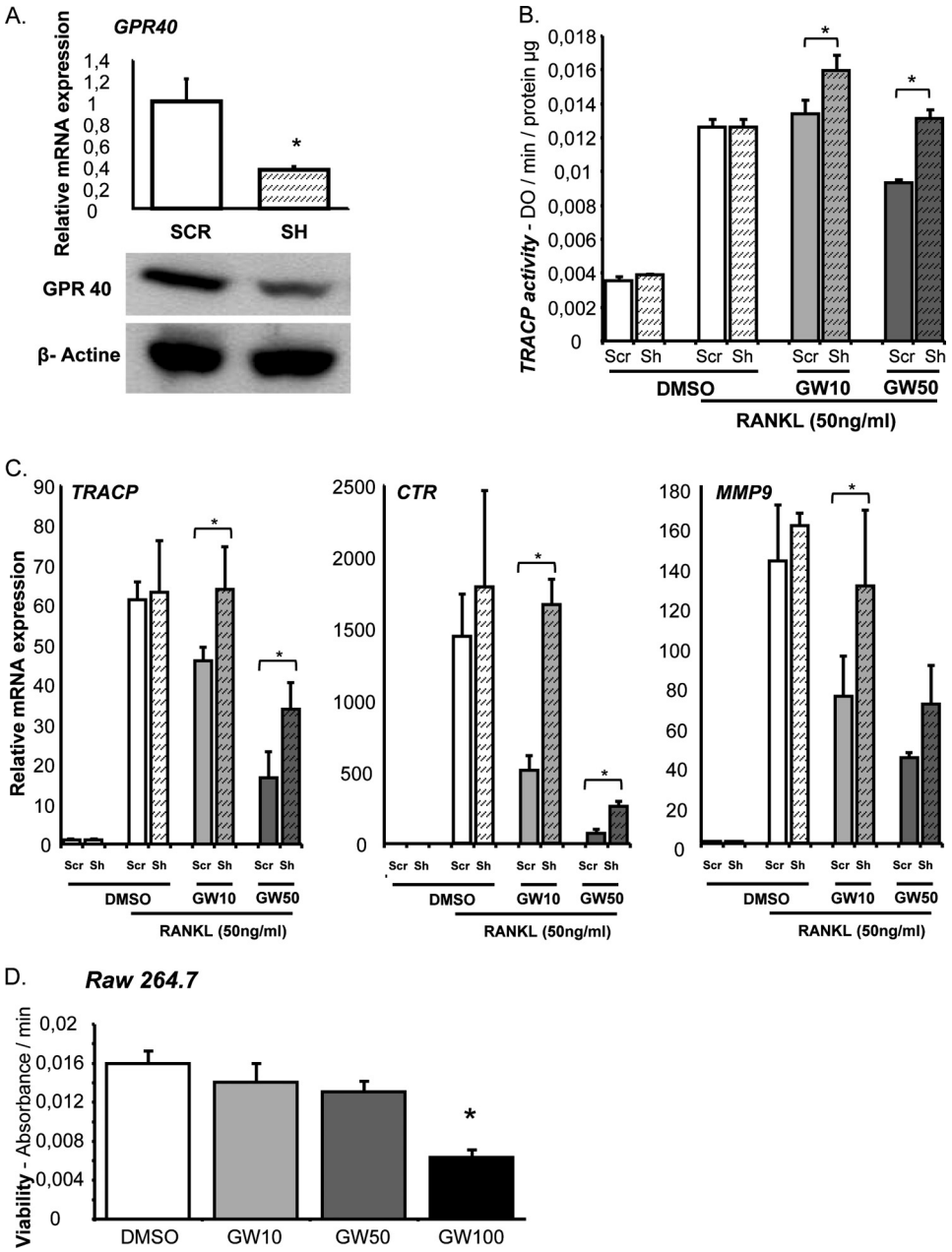

FIGURE 3. **GW9508 inhibits RANKL-induced osteoclastogenesis in RAW264.7 cell cultures.** *A*, RT-PCR and Western blot analysis. Cells were invalidated for GPR40 expression (*Sh*) or transfected with a nontargeting vector (*SCR*). *B*, TRACP enzymatic activity. Osteoclast differentiation was induced by murine recombinant RANKL (50 ng/ml). DMSO was used as a vehicle. GPR40 agonist GW9508 was used at either 10 or 50 μM (GW10 or GW50). *C*, osteoclast marker expression analyzed by real-time RT-PCR. GPR40 agonist GW9508 was used at either 10 or 50 μM. *, $p < 0.05$. *D*, XTT cell viability assay. *, $p < 0.05$ *versus* DMSO control; *error bars* represent standard deviation (±S.D.).

software; Microsoft Office 2007). * represents significant differences: ($p < 0.05$). Different letters are attributed to statistically different groups ($a \neq b \neq c \ldots ; p < 0.05$).

RESULTS

Lack of GPR40 Is Associated with Bone Loss—Using a whole body GPR40 knock-out mouse model (19), we investigated its potential role in bone using micro-CT analysis. GPR40$^{-/-}$ mice exhibited osteoporotic features with reduced bone mineral density, bone volume, and altered microarchitecture (Fig. 1*A* and *B*), suggesting a positive role of GPR40 on bone.

To further investigate this hypothesis, we examined the expression of GPR40 in bone tissue to determine whether GPR40 may directly influence bone cell activities. As shown in Fig. 1*C*, GPR40 protein expression was confirmed in wild-type mice but not in GPR40$^{-/-}$ littermates.

GPR40 Agonist GW9508 Inhibits RANKL-induced Osteoclast Differentiation—Using primary bone marrow macrophage cultures and the osteoclast precursor cell line RAW264.7 we confirmed the expression of GPR40 in osteoclasts and tested the effects of GW9508, a GPR40 agonist (27), on RANKL-induced osteoclastogenesis.

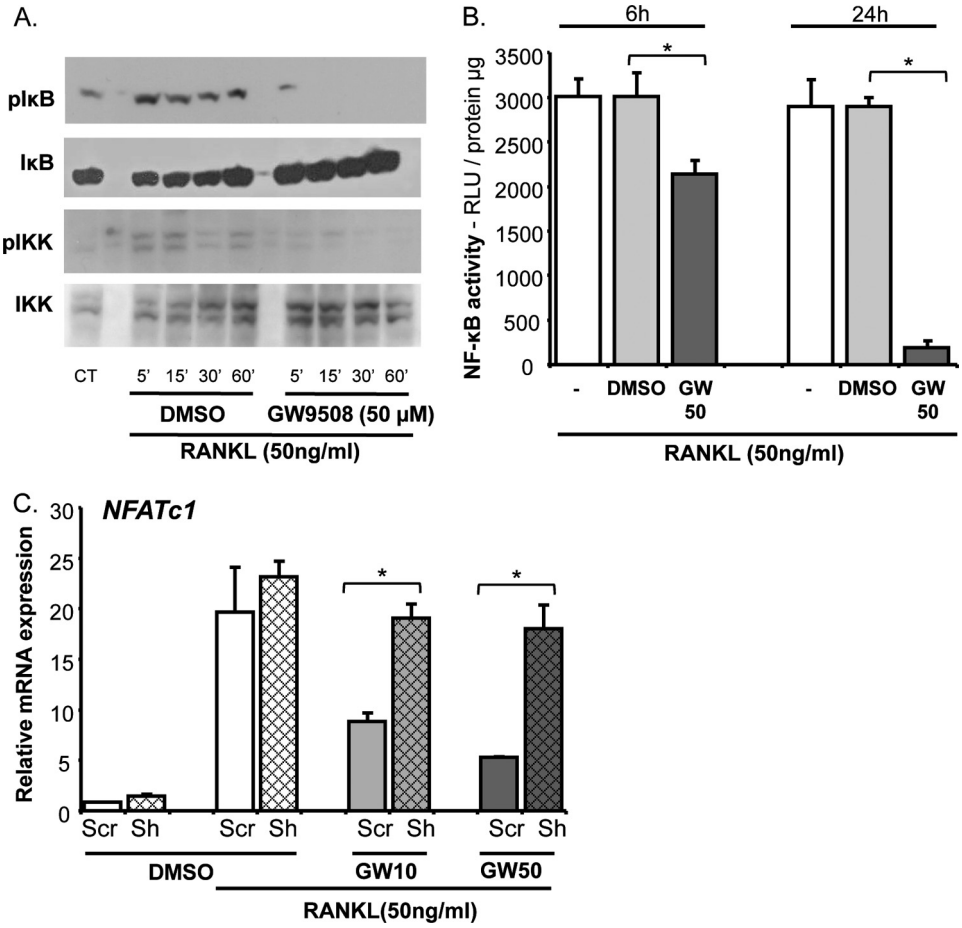

FIGURE 4. **GW9508 inhibits RANKL-induced signaling pathways in RAW264.7 cell cultures.** *A*, Western blot analysis of IkBα and IKKα/β phosphorylation. *B*, NF-κB-dependent luciferase assay. DMSO was used as a vehicle. GPR40 agonist GW9508 was used at 50 μM (GW50). Relative light units were measured at 6 and 24 h after incubation and reported to total protein content. *C*, NFATc1 expression analyzed by real-time RT-PCR in cells invalidated for GPR40 expression (*Sh*) or transfected with a nontargeting vector (*SCR*). *, $p < 0.05$. DMSO was used as a vehicle. GPR40 agonist GW9508 was used at either 10 or 50 μM (GW10 or GW50). *Error bars* represent standard deviation (±S.D.).

Addition of RANKL induced the formation of giant, multinucleated TRACP-positive osteoclasts, in both wild-type and GPR40$^{-/-}$ bone marrow cells. This RANKL induction was blocked by GW9508; however, inhibition of osteoclastogenesis occurred in wild-type but not in GPR40$^{-/-}$ cells (Fig. 2*A* and *B*). Accordingly, GW9508 reduced the expression of the osteoclast markers TRACP, calcitonin receptor (CTR), matrix metalloproteinase-9 (MMP-9) and cathepsin K (CatK) induced by RANKL in wild-type, but not GPR40$^{-/-}$ cells (Fig. 2*C*).

We further confirmed these observations in RAW264.7 cells as a pre-osteoclast cell line model. GPR40 expression was knocked down in RAW264.7 cells using stable shRNA interference (Fig. 3*A*). Inhibition of GPR40 was routinely estimated around 60% at both mRNA and protein. Similar to our observations in bone marrow cultures, we found that GW9508 significantly altered TRACP activity as measured by enzymatic assay in scrambled cultures but not in GPR40 knocked-down cells (Fig. 3*B*). These data are reinforced by osteoclast marker expression analyses, thus validating both the hypothesis and the model (Fig. 3*C*). Importantly, GW9508 inhibition of osteoclastogenesis was not related to cytotoxicity within the range of concentration used, thus supporting a specific effect of the GPR40 agonist on cell differentiation at 10 and 50 μM (Fig. 3*D*).

GW9508 Down-regulates Osteoclastogenesis by Blocking RANKL-induced Signaling Pathways—To identify the molecular targets linking GPR40 activation to inhibition of osteoclast differentiation, we measured RANKL-induced signaling pathways. The main downstream pathway for RANK activation is the NF-κB system. Interestingly, GW9508 abrogated RANKL-induced phosphorylation of Inhibitor of κBα (IκBα) and IκB Kinase (IKKα/β) (Fig. 4*A*), suggesting that GW9508 prevents NF-κB activation, nuclear translocation and subsequent transcriptional activity. Indeed, using RAW264.7 cell cultures transfected with a luciferase reporter construct under the control of NF-κB response-elements, incubation with GW9508 in the presence of RANKL led to a marked decrease in luciferase activity, thus further supporting a global inhibition of the NF-κB pathway (Fig. 4*B*). Consequently (28), NFATc1 expression was found altered by GW9508. Nevertheless, GW9508 had no effect on NFATc1 expression when GPR40 was knocked downed, confirming a GPR40-dependent mechanism (Fig. 4*C*).

GW9508 GPR40-dependently Counteracts Bone Loss in Vivo—To examine the bone-protective effect of the GPR40 agonist *in vivo*, mice were ovariectomized to induce bone loss and were given GW9508 or DMSO (as a vehicle) orally. Administration of GW9508 prevented the alterations in bone micro-

A.

	Sham DMSO	OVX DMSO	OVX GW
BV/TV (%)	**10.992 ± 2.041** [a]	**7.381 ± 1.174** [b]	**10.011 ± 1.473** [a]
Tb.Th (mm)	0,231 ± 0,029	0,205 ± 0,014	0,221 ± 0,027
Tb.N (1/mm)	0,482 ± 0,109 [a]	0,361 ± 0,059 [b]	0,457 ± 0,09 [ab]
Tb.Sp (mm)	**1,919 ± 0,407** [a]	**2,625 ± 0,436** [b]	**2,026 ± 0,373** [a]
Bone surface density (1/mm)	7.501 ± 0.184 [a]	5.468 ± 1.001 [b]	6.724 ± 0.18 [ab]

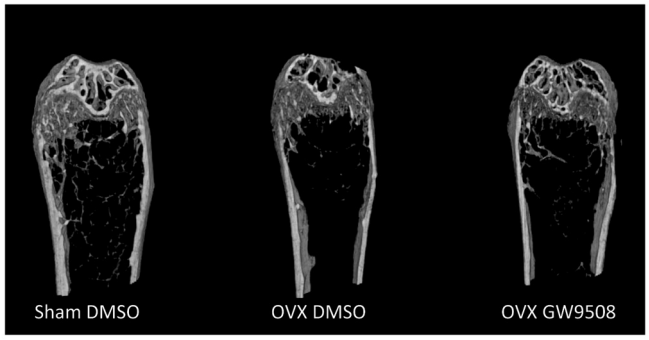

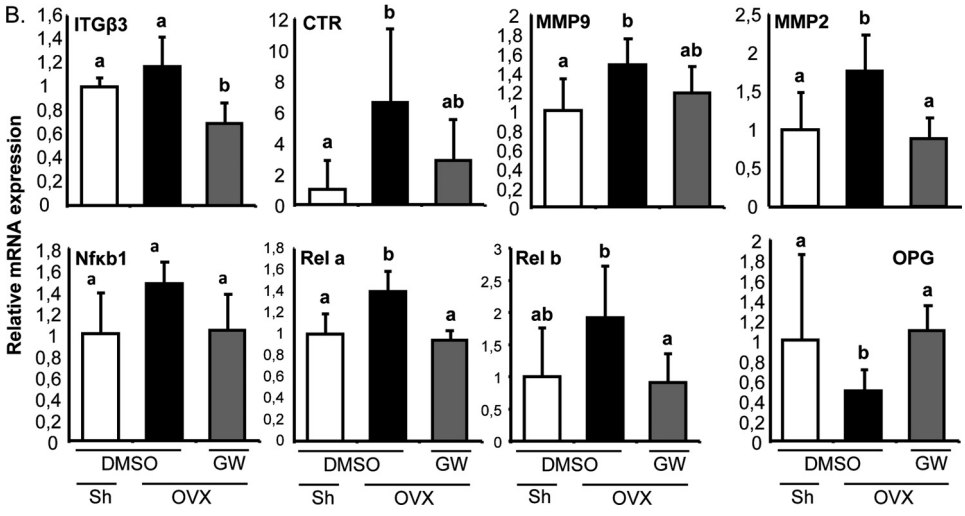

FIGURE 5. **GPR40 agonist as a protective agent against *in vivo* OVX-induced bone loss.** *A*, bone microarchitecture (females; *OVX*, ovariectomy; *Sh*, Sham-operated; 14-week-old mice; $n = 7$ per group; *BV/TV*, bone volume/total volume; *Tb.N*, trabecular number; *Tb.Sp*, trabecular spaces; *Tb.Th*, trabecular thickness). Mice received either DMSO as vehicle or GPR40 agonist GW9508 (8 mg/kg of body weight: *GW*). *B*, representative bone tissue marker expression analyzed by TLDA on whole tibiae (Applied Biosystems 7900HT real-time PCR system). Tissues were collected from OVX or Sham-operated mice that received either DMSO as vehicle or GPR40 agonist GW9508 (8 mg/kg of body weight: GW). Different *letters* are attributed to significantly different groups ($p < 0.05$); *error bars* represent standard deviation (±S.D.).

architecture observed upon OVX (Fig. 5*A*). Accordingly, transcriptomic analyses of whole tibiae showed a decrease in osteoclast marker expression, whereas osteoprotegerin expression, a natural decoy receptor for RANKL, was preserved (Fig. 5*B*), thus confirming that differentiation of the resorbing cells is targeted by the GPR40 agonist. On the other hand, body composition analyses revealed that, without significantly affecting either daily food intake (Fig. 6*A*), body weight or lean body mass (Fig. 6, *B* and *C*), GW9508 administration counteracted the fat mass gain associated with bone loss (Fig. 6*D*). These observations strongly support that prevention of bone loss is not related to bone stimulation by mechanical loading. Most importantly, the bone-sparing effect of GW9508 did not occur in GPR40$^{-/-}$ mice (Fig. 6*E*).

DISCUSSION

Besides their biological effects on the function of various cell types through their intracellular metabolism, long chain fatty acids activate the membrane-bound receptor GPR40. Our results show for the first time in a GPR40$^{-/-}$ mouse model that GRP40 plays a crucial role in osteoclast biogenesis and subsequent bone remodeling.

Cornish *et al.* (24) showed that RAW264.7 cells express both GPR120 and GPR40 at the mRNA levels and hypothesized a potential role of these receptors in the effects of saturated fatty acids on osteoclastogenesis. In addition, Oh *et al.* (23) recently demonstrated that GPR120 was responsible for mediating docosahexaenoic acid anti-inflammatory properties in a macrophage

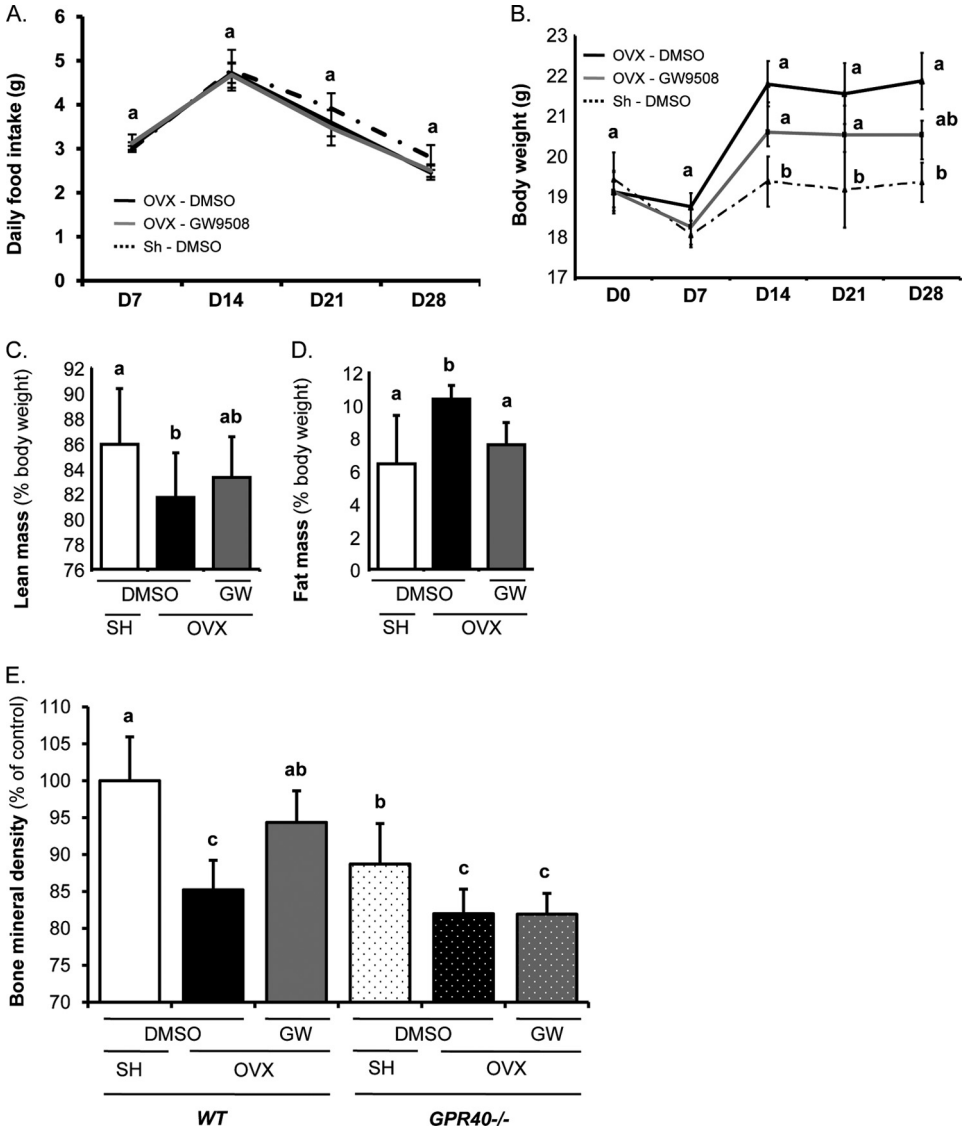

FIGURE 6. **GW9508 protective effect on bone is dependent on GPR40 expression.** *A*, food intake. Consumption was analyzed weekly throughout the protocol. *B*, mouse body weight. Mice were weighed every week throughout the experimental period. *C* and *D*, EchoMRI body composition analysis. Mice received either DMSO as vehicle or GPR40 agonist GW9508 (8 mg/kg of body weight: GW). *E*, bone mineral density (females; *OVX*, ovariectomy; *SH*, Sham-operated; 14-week-old mice; $n = 7$/group; wild-type (WT) *versus* GPR40$^{-/-}$ mice). Different *letters* are attributed to significantly different groups ($p < 0.05$); *error bars* represent standard deviation (±S.D.).

differentiation system. In contrast to our results, Oh *et al.* did not observe GPR40 expression in RAW264.7 cells. However, they used a macrophage differentiation protocol rather than an osteoclast differentiation procedure. In the present study, we confirm expression of GPR40 at both the mRNA and protein level in bone cells from hematopoietic origin and demonstrate its crucial role on bone resorption both *in vitro* and *in vivo*.

Consistent with the bone phenotype in GPR40$^{-/-}$ mice, *ex vivo* and *in vitro* invalidation experiments demonstrated that GPR40 is required for GW9508 inhibition of osteoclastogenesis. Furthermore, GW9508 failed to protect GPR40$^{-/-}$ ovariectomized mice from bone loss. These results clearly demonstrate the essential role of GPR40 in regulating osteoclast behavior and suggest its potential as a target for new therapeutic and nutritional strategies to counter bone loss. However, although osteoblast markers do not seem to be impacted by GPR40 (data not shown), further *in vivo* investigations are required to decipher the contribution of GPR40 agonist in bone-forming cell activities.

We used a mice model with a global deletion of GPR40. Thus, the bone phenotype *in vivo* may also result from GPR40 invalidation in other organs known to influence bone metabolism. Indeed, GPR40 mediates the insulin-secretory effect of fatty acids, and insulin is an anabolic agent known to stimulate osteoblast function. Thus, lower levels of circulating insulin in whole body GPR40$^{-/-}$ mice could conceivably contribute to the observed osteoporotic features (29). However, as demonstrated in both primary and cell line cultures, GPR40 was expressed and required to mediate inhibition of cell differentiation in the presence of a GPR40 agonist *ex vivo*. These data correlate with the osteoporotic phenotype of GPR40$^{-/-}$ mice; and without excluding possible indirect effects of insulin, they strongly support a direct role of GPR40 on osteoclast differentiation and function.

GPR40 shares the ability to bind long chain fatty acids with TLRs and PPARs (10–13, 30, 31). The effects of PPARs on osteoclastogenesis remain controversial and depend on the receptor subtype. PPARγ activation was found either to inhibit (32, 33) or stimulate (34) osteoclast differentiation, whereas antisense strategies for PPARδ/β revealed a pro-resorbing impact of these two isoforms (35). Interestingly, PPARγ agonists such as thiazolidinediones and rosiglitazone also stimulate GPR40 signaling pathways, therefore inhibition of osteoclastogenesis by PPARγ activators may in fact result from an uninvestigated GPR40 activation (25, 36, 37).

Jonhson *et al.* (14) reported that mice deficient for TLR4 exhibit increased bone size and bone mineral content and density. Consistently, saturated fatty acids have been shown to increase activation of NF-κB and subsequent bone resorption via TLR4 in osteoclasts (38). In contrast, in the present study we observed that the inhibitory effect of GW9508 on NF-κB transcriptional activity was GPR40-dependent similar to the GPR120-dependent anti-inflammatory effect of docosahexaenoic acid as demonstrated by Oh *et al.* in macrophages (23).

The recent results of phase 2 clinical trials revealed that a GPR40 agonist (TAK-875) is highly effective in lowering blood glucose levels in patients with type 2 diabetes without inducing iatrogenic hypoglycemia (20, 21). Therefore, in a context of growing prevalence of metabolic and age-related disorders, our results showing the key role of GPR40 in mediating inhibition of osteoclastogenesis and the ability of a GPR40 agonist to protect from bone loss *in vivo* suggest that prevention of bone complications could be an additional benefit of this class of drugs.

Acknowledgment—We thank Amgen Inc., Thousand Oaks, CA, for the GPR40$^{-/-}$ mice.

REFERENCES

1. Ono, K., Kaneko, H., Choudhary, S., Pilbeam, C. C., Lorenzo, J. A., Akatsu, T., Kugai, N., and Raisz, L. G. (2005) Biphasic effect of prostaglandin E2 on osteoclast formation in spleen cell cultures: role of the EP2 receptor. *J. Bone Miner. Res.* **20,** 23–29
2. Tsutsumi, R., Xie, C., Wei, X., Zhang, M., Zhang, X., Flick, L. M., Schwarz, E. M., and O'Keefe, R. J. (2009) PGE2 signaling through the EP4 receptor on fibroblasts upregulates RANKL and stimulates osteolysis. *J. Bone Miner. Res.* **24,** 1753–1762
3. Laneuville, O., Breuer, D. K., Xu, N., Huang, Z. H., Gage, D. A., Watson, J. T., Lagarde, M., DeWitt, D. L., and Smith, W. L. (1995) Fatty acid substrate specificities of human prostaglandin-endoperoxide H synthase-1 and -2: formation of 12-hydroxy-(9*Z*, 13*E*/*Z*, 15*Z*)- octadecatrienoic acids from α-linolenic acid. *J. Biol. Chem.* **270,** 19330–19336
4. Raisz, L. G., Alander, C. B., and Simmons, H. A. (1989) Effects of prostaglandin E3 and eicosapentaenoic acid on rat bone in organ culture. *Prostaglandins* **37,** 615–625
5. Corwin, R. L. (2003) Effects of dietary fats on bone health in advanced age. *Prostaglandins Leukot. Essent. Fatty Acids* **68,** 379–386
6. Calder, P. C. (2006) *n*-3 polyunsaturated fatty acids, inflammation, and inflammatory diseases. *Am. J. Clin. Nutr.* **83,** 1505S–1519S
7. Diascro, D. D., Jr., Vogel, R. L., Johnson, T. E., Witherup, K. M., Pitzenberger, S. M., Rutledge, S. J., Prescott, D. J., Rodan, G. A., and Schmidt, A. (1998) High fatty acid content in rabbit serum is responsible for the differentiation of osteoblasts into adipocyte-like cells. *J. Bone Miner. Res.* **13,** 96–106
8. Maurin, A. C., Chavassieux, P. M., and Meunier, P. J. (2005) Expression of PPARγ and β/γ in human primary osteoblastic cells: influence of polyunsaturated fatty acids. *Calcif. Tissue Int.* **76,** 385–392
9. Jeon, M. J., Kim, J. A., Kwon, S. H., Kim, S. W., Park, K. S., Park, S. W., Kim, S. Y., and Shin, C. S. (2003) Activation of peroxisome proliferator-activated receptor-γ inhibits the Runx2-mediated transcription of osteocalcin in osteoblasts. *J. Biol. Chem.* **278,** 23270–23277
10. Hwang, D. (2001) Modulation of the expression of cyclooxygenase-2 by fatty acids mediated through Toll-like receptor 4-derived signaling pathways. *FASEB J.* **15,** 2556–2564
11. Shi, H., Kokoeva, M. V., Inouye, K., Tzameli, I., Yin, H., and Flier, J. S. (2006) TLR4 links innate immunity and fatty acid-induced insulin resistance. *J. Clin. Invest.* **116,** 3015–3025
12. Coenen, K. R., Gruen, M. L., Lee-Young, R. S., Puglisi, M. J., Wasserman, D. H., and Hasty, A. H. (2009) Impact of macrophage Toll-like receptor 4 deficiency on macrophage infiltration into adipose tissue and the artery wall in mice. *Diabetologia* **52,** 318–328
13. Himes, R. W., and Smith, C. W. (2010) Tlr2 is critical for diet-induced metabolic syndrome in a murine model. *FASEB J.* **24,** 731–739
14. Johnson, G. B., Riggs, B. L., and Platt, J. L. (2004) A genetic basis for the "Adonis" phenotype of low adiposity and strong bones. *FASEB J.* **18,** 1282–1284
15. Briscoe, C. P., Tadayyon, M., Andrews, J. L., Benson, W. G., Chambers, J. K., Eilert, M. M., Ellis, C., Elshourbagy, N. A., Goetz, A. S., Minnick, D. T., Murdock, P. R., Sauls, H. R., Jr., Shabon, U., Spinage, L. D., Strum, J. C., Szekeres, P. G., Tan, K. B., Way, J. M., Ignar, D. M., Wilson, S., and Muir, A. I. (2003) The orphan G protein-coupled receptor GPR40 is activated by medium and long chain fatty acids. *J. Biol. Chem.* **278,** 11303–11311
16. Itoh, Y., Kawamata, Y., Harada, M., Kobayashi, M., Fujii, R., Fukusumi, S., Ogi, K., Hosoya, M., Tanaka, Y., Uejima, H., Tanaka, H., Maruyama, M., Satoh, R., Okubo, S., Kizawa, H., Komatsu, H., Matsumura, F., Noguchi, Y., Shinohara, T., Hinuma, S., Fujisawa, Y., and Fujino, M. (2003) Free fatty acids regulate insulin secretion from pancreatic beta cells through GPR40. *Nature* **422,** 173–176
17. Kotarsky, K., Nilsson, N. E., Olde, B., and Owman, C. (2003) Progress in methodology: improved reporter gene assays used to identify ligands acting on orphan seven-transmembrane receptors. *Pharmacol. Toxicol.* **93,** 249–258
18. Covington, D. K., Briscoe, C. A., Brown, A. J., and Jayawickreme, C. K. (2006) The G-protein-coupled receptor 40 family (GPR40-GPR43) and its role in nutrient sensing. *Biochem. Soc. Trans.* **34,** 770–773
19. Latour, M. G., Alquier, T., Oseid, E., Tremblay, C., Jetton, T. L., Luo, J., Lin, D. C., and Poitout, V. (2007) GPR40 is necessary but not sufficient for fatty acid stimulation of insulin secretion *in vivo*. *Diabetes* **56,** 1087–1094
20. Araki, T., Hirayama, M., Hiroi, S., and Kaku, K. (2012) GPR40-induced insulin secretion by the novel agonist TAK-875: first clinical findings in patients with type 2 diabetes. *Diabetes Obes. Metab.* **14,** 271–278
21. Burant, C. F., Viswanathan, P., Marcinak, J., Cao, C., Vakilynejad, M., Xie, B., and Leifke, E. (2012) TAK-875 *versus* placebo or glimepiride in type 2 diabetes mellitus: a phase 2, randomised, double-blind, placebo-controlled trial. *Lancet* **379,** 1403–1411
22. Nilsson, N. E., Kotarsky, K., Owman, C., and Olde, B. (2003) Identification of a free fatty acid receptor, FFA2R, expressed on leukocytes and activated by short-chain fatty acids. *Biochem. Biophys. Res. Commun.* **303,** 1047–1052
23. Oh, D. Y., Talukdar, S., Bae, E. J., Imamura, T., Morinaga, H., Fan, W., Li, P., Lu, W. J., Watkins, S. M., and Olefsky, J. M. (2010) GPR120 is an ω-3 fatty acid receptor mediating potent anti-inflammatory and insulin-sensitizing effects. *Cell* **142,** 687–698
24. Cornish, J., MacGibbon, A., Lin, J. M., Watson, M., Callon, K. E., Tong, P. C., Dunford, J. E., van der Does, Y., Williams, G. A., Grey, A. B., Naot, D., and Reid, I. R. (2008) Modulation of osteoclastogenesis by fatty acids. *Endocrinology* **149,** 5688–5695
25. Mieczkowska, A., Baslé, M. F., Chappard, D., and Mabilleau, G. (2012) Thiazolidinediones induce osteocyte apoptosis by a G protein-coupled receptor 40-dependent mechanism. *J. Biol. Chem.* **287,** 23517–23526
26. Wittrant, Y., Gorin, Y., Woodruff, K., Horn, D., Abboud, H. E., Mohan, S., and Abboud-Werner, S. L. (2008) High D$^+$glucose concentration inhibits RANKL-induced osteoclastogenesis. *Bone* **42,** 1122–1130

27. Briscoe, C. P., Peat, A. J., McKeown, S. C., Corbett, D. F., Goetz, A. S., Littleton, T. R., McCoy, D. C., Kenakin, T. P., Andrews, J. L., Ammala, C., Fornwald, J. A., Ignar, D. M., and Jenkinson, S. (2006) Pharmacological regulation of insulin secretion in MIN6 cells through the fatty acid receptor GPR40: identification of agonist and antagonist small molecules. *Br. J. Pharmacol.* **148,** 619–628
28. Asagiri, M., Sato, K., Usami, T., Ochi, S., Nishina, H., Yoshida, H., Morita, I., Wagner, E. F., Mak, T. W., Serfling, E., and Takayanagi, H. (2005) Autoamplification of NFATc1 expression determines its essential role in bone homeostasis. *J. Exp. Med.* **202,** 1261–1269
29. Alquier, T., Peyot, M. L., Latour, M. G., Kebede, M., Sorensen, C. M., Gesta, S., Ronald Kahn, C., Smith, R. D., Jetton, T. L., Metz, T. O., Prentki, M., and Poitout, V. (2009) Deletion of GPR40 impairs glucose-induced insulin secretion *in vivo* in mice without affecting intracellular fuel metabolism in islets. *Diabetes* **58,** 2607–2615
30. Berger, J., Bailey, P., Biswas, C., Cullinan, C. A., Doebber, T. W., Hayes, N. S., Saperstein, R., Smith, R. G., and Leibowitz, M. D. (1996) Thiazolidinediones produce a conformational change in peroxisomal proliferator-activated receptor-γ: binding and activation correlate with antidiabetic actions in db/db mice. *Endocrinology* **137,** 4189–4195
31. Still, K., Grabowski, P., Mackie, I., Perry, M., and Bishop, N. (2008) The peroxisome proliferator-activator receptor α/δ agonists linoleic acid and bezafibrate upregulate osteoblast differentiation and induce periosteal bone formation *in vivo*. *Calcif. Tissue Int.* **83,** 285–292
32. Chan, B. Y., Gartland, A., Wilson, P. J., Buckley, K. A., Dillon, J. P., Fraser, W. D., and Gallagher, J. A. (2007) PPAR agonists modulate human osteoclast formation and activity *in vitro*. *Bone* **40,** 149–159
33. Hounoki, H., Sugiyama, E., Mohamed, S. G., Shinoda, K., Taki, H., Abdel-Aziz, H. O., Maruyama, M., Kobayashi, M., and Miyahara, T. (2008) Activation of peroxisome proliferator-activated receptor γ inhibits TNF-α-mediated osteoclast differentiation in human peripheral monocytes in part via suppression of monocyte chemoattractant protein-1 expression. *Bone* **42,** 765–774
34. Wan, Y., Chong, L. W., and Evans, R. M. (2007) PPAR-γ regulates osteoclastogenesis in mice. *Nat. Med.* **13,** 1496–1503
35. Mano, H., Kimura, C., Fujisawa, Y., Kameda, T., Watanabe-Mano, M., Kaneko, H., Kaneda, T., Hakeda, Y., and Kumegawa, M. (2000) Cloning and function of rabbit peroxisome proliferator-activated receptor δ/β in mature osteoclasts. *J. Biol. Chem.* **275,** 8126–8132
36. Smith, N. J., Stoddart, L. A., Devine, N. M., Jenkins, L., and Milligan, G. (2009) The action and mode of binding of thiazolidinedione ligands at free fatty acid receptor 1. *J. Biol. Chem.* **284,** 17527–17539
37. Gras, D., Chanez, P., Urbach, V., Vachier, I., Godard, P., and Bonnans, C. (2009) Thiazolidinediones induce proliferation of human bronchial epithelial cells through the GPR40 receptor. *Am. J. Physiol. Lung Cell Physiol.* **296,** L970–978
38. Oh, S. R., Sul, O. J., Kim, Y. Y., Kim, H. J., Yu, R., Suh, J. H., and Choi, H. S. (2010) Saturated fatty acids enhance osteoclast survival. *J. Lipid Res.* **51,** 892–899